Asian Journal of Pharmaceutical Sciences 18 (2023) 100826

Available online at www.sciencedirect.com

ScienceDirect

journal homepage: www.elsevier.com/locate/AJPS

Original Research Paper

CD71-mediated liposomal arsenic-nickel complex combined with all-trans retinoic acid for the efficacy of acute promyelocytic leukemia

Xiao Liu[a], *Lili Zhang*[a,b], *Yueying Yang*[a], *Weiwei Yin*[a], *Yunhu Liu*[a], *Chunyi Luo*[a], *Ruizhe Zhang*[a], *Zhiguo Long*[c,*], *Yanyan Jiang*[a,*], *Bing Wang*[b,d,*]

[a] *Key Laboratory of Smart Drug Delivery, Ministry of Education, Department of Pharmaceutics, School of Pharmacy, Fudan University, Shanghai 201023, China*

[b] *School of Pharmacy, Shanghai University of Traditional Chinese Medicine, Shanghai 201203, China*

[c] *Department of Hematology, Shanghai Pudong Hospital, Fudan University, Shanghai 201399, China*

[d] *Shanghai Institute of Materia Medica, Chinese Academy of Sciences, Shanghai 201203, China*

ARTICLE INFO

Article history:
Received 9 December 2022
Revised 9 April 2023
Accepted 9 June 2023
Available online 7 July 2023

Keywords:
Transferrin
Arsenic trioxide
Acute promyelocytic leukemia
All-trans retinoic acid
Liposome

ABSTRACT

Clinically, arsenic trioxide (ATO) was applied to the treatment of acute promyelocytic leukemia (APL) as a reliable and effective frontline drug. However, the administration regimen of As^{III} was limited due to its fast clearance, short therapeutic window and toxicity as well. Based on CD71 overexpressed on APL cells, in present study, a transferrin (Tf)-modified liposome (LP) was established firstly to encapsulate As^{III} in arsenic-nickel complex by nickel acetate gradient method. The As^{III}-loaded liposomes (AsLP) exhibited the feature of acid-sensitive release *in vitro*. Tf-modified AsLP (Tf-AsLP) were specifically taken up by APL cells and the acidic intracellular environment triggered liposome to release As^{III} which stimulated reactive oxygen species level and caspase-3 activity. Tf-AsLP prolonged half-life of As^{III} in blood circulation, lowered systemic toxicity, and promoted apoptosis and induced cell differentiation at lesion site *in vivo*. Considering that ATO combined with RA is usually applied as the first choice in clinic for APL treatment to improve the therapeutic effect, accordingly, a Tf-modified RA liposome (Tf-RALP) was designed to reduce the severe side effects of free RA and assist Tf-AsLP for better efficacy. As expected, the tumor inhibition rate of Tf-AsLP was improved significantly with the combination of Tf-RALP on subcutaneous tumor model. Furthermore, APL orthotopic NOD/SCID mice model was established by ^{60}CO irradiation and HL-60 cells intravenously injection. The effect of co-administration (Tf-AsLP + Tf-RALP) was also confirmed to conspicuous decrease the number of leukemia cells in the circulatory system and prolong the survival time of APL mice by promoting the

* Corresponding authors.
E-mail addresses: zglong1976@126.com (Z. Long), yanyanjiang@fudan.edu.cn (Y. Jiang), bwang@simm.ac.cn (B. Wang).
Peer review under responsibility of Shenyang Pharmaceutical University.

https://doi.org/10.1016/j.ajps.2023.100826

APL cells' apoptosis and differentiation in peripheral blood and bone marrow. Collectively, Tf-modified acid-sensitive AsLP could greatly reduce the systemic toxicity of free drug. Moreover, Tf-AsLP combined with Tf-RALP could achieve better efficacy. Thus, transferrin-modified As^{III} liposome would be a novel clinical strategy to improve patient compliance, with promising translation prospects.

1. Introduction

Acute promyelocytic leukemia (APL), morphologically classified as acute myeloid leukemia-M3 (AML-M3) by French-American-British classification, was a unique subtype of AML with specific biological and clinical features including cytopenias and disseminated intravascular coagulation (DIC). It was characterized by abnormal proliferation of promyelocytes in the bone marrow (BM) with a reciprocal translocation of t (15;17). The gene translocation brought about the expression of promyelocytic leukemia-retinoic acid receptor-α (PML-RARα) fusion protein which blocked the transcription and differentiation of granulocytes, leading to uncontrolled proliferation [1,2].

Clinically, all-trans retinoic acid (RA) was first proven effective in 1988 with a complete remission rate exceeding 90% for APL therapy [3]. But the remission was not prolonged under the condition of using RA alone because of a quick relapse. Besides, RA induced differentiation syndrome in the initial studies, causing unexplained fever, hypotension, respiratory distress and other symptoms on lung, kidney, pleura and pericardium [4,5]. Thus, RA along with chemotherapy became the gold standard in front-line treatment of APL.

Arsenic trioxide (ATO, As_2O_3), a naturally metalloid compound, and its various forms have been used in ancient China for over 2,000 years [6]. In 1994, clinical trials began using pure ATO in Shanghai and Harbin Medical Universities. In 1999, Arsenious Acid and Sodium Chloride Injection (main ingredient: H_3AsO_3) was firstly approved in China which was considered as breakthrough in treating relapsed APL patients. And then, Trisenox, the injectable form of ATO, was approved by the FDA as frontline drug for the relapsed and refractory APL. It was proved *in vitro* that ATO at a low concentration (0.25-0.5 μM) could promote the normal differentiation of APL cells [7]. While ATO at a higher concentration (1-2 μM) induced the generation of intracellular reactive oxygen species (ROS) and reduced the content of glutathione, leading to cellular DNA and RNA damage of APL cells [8]. The ATO level in blood was clinically recognized as a key factor determining efficacy or toxicity.

As the medicinal form of ATO, As^{III} was widely used in the treatment of APL. However, free As^{III} in injection was cleared rapidly from the blood in relapsed APL patients ($T_{1/2\alpha}$, 0.89 ± 0.29 h and $T_{1/2\beta}$, 12.13 ± 3.31 h) [9]. Increasing dosage of As^{III} for meeting the treating requirement might lead to severe toxicity to all vital organs of human body, especially heart and liver [10]. Therefore, arsenite injection in clinical administration was required for an intravenously infusing at a relatively slow speed in order to control a constant therapeutic blood level for maximizing efficacy and minimizing toxicity. Even so, due to this long-term infusion and obvious individual differences, As^{III} clinical treatment still cannot completely overcome these limitations.

Liposomes (LP) encapsulating cytotoxic drugs possessed promising properties on biocompatibility, long-time circulation and low toxicity than free drug. Modification of surface targets on LP by chemical synthesis, physical coating, electrostatic adsorption, etc. could improve the selectivity and efficacy [11,12]. CD71, also named transferrin receptor-1 (TfR-1), was present in all over-proliferating cells, which could serve as a diagnostic marker for APL on detecting and isolating myeloblasts in blood [13]. According to this feature, transferrin (Tf), an endogenous chelator with serum iron transportation, was appropriate in targeting APL cells *in vivo* [14].

In present study, a Tf-modified LP was firstly applied as a carrier for encapsulating As^{III} to overcome the shortcomings of ATO injection in clinic, including fast clearance, high toxicity and poor compliance. As shown in Scheme 1, ATO in As^{III} form was entrapped into liposomal vesicles by nickel acetate gradient method and Tf was modified on the surface to obtain Tf-AsLP. The target function on HL-60 cells and toxicity to peripheral blood cells were investigated, together with the efficacy and mechanism of Tf-AsLP in promoting the apoptosis and differentiation of HL-60 cells or other leukemic cells through *in vitro* assays. To explored the efficacy *in vivo*, Tf-AsLP was evaluated via subcutaneous mice model and orthotopic leukemia mice model, respectively. And the safety was simultaneously assessed on peripheral blood cells and tissues. Considering that ATO combined with RA is usually adopt in clinic to obtain better curative effect and lower recurrence rate, Tf-modified liposomes was also applied as the carrier to encapsulate RA to reduce drug resistance and side effects of free drug. More importantly, the administration of Tf-AsLP combined with Tf-RALP was performed in pharmacodynamics experiments for better efficacy.

2. Materials and methods

2.1. *Materials*

DSPE-PEG2000, DSPE-PEG2000-COOH, cholesterol (CHO) and DSPC were obtained from Shanghai AVT Pharmaceutical Technology Co., Ltd. (Shanghai, China), and they're all medicated injection grade. ATO provided by Sinopharm

Chemical Reagent Co., Ltd was dissolved in about 2 M of NaOH solution, and the pH was adjusted to 9.0 to form the As^{III} solution. Tf (purity: 100%), N-hydroxysulfosuccinimide (Sulfo-NHS, purity > 99%), 4-morpholineethanesulfonic acid (MES, purity > 99%) were obtained from Meilun Biotechnology Co., Ltd. (Dalian, China). EDC·HCl (purity ≥ 99%) was obtained from Shanghai Medpep Co., Ltd. (Shanghai, China). RA, Poly-L-lysine (PLL), LysoTracker Red, Sephadex G-50 were obtained from Sigma-Aldrich (St. Louis, MO, USA). Nickel(II) acetate tetrahydrate ($Ni(OAc)_2$, purity ≥98.0%), Sodium chloride (NaCl, purity ≥ 99.8%) and HEPES (purity ≥ 99.5%) were purchased from Sinopharm Chemical Reagent Co.,Ltd. All other materials were of analytical grade.

2.2. *Preparation of liposomal [AsIII, NiII] complexes*

The As^{III}-loaded liposomes (AsLP) were prepared using a nickel acetate ($Ni(OAc)_2$) gradient method. DSPC, CHO and DSPE-PEG2000 (2: 1: 0.2, molar ratio) were dissolved completely in the solvent of methanol and chloroform (1:4, v/v) and dried at 45 °C under vacuum. Hydrated the lipid film with 300 mM $Ni(OAc)_2$ solution at 55 °C for 60 min, and treated with an ultrasonic probe (Xinyi Ultrasonic Equipment LTD, Ningbo, China) for 10 min at 80 W to yield unilamellar Ni^{II}-encapsulated liposomes (LP). The extraliposomal $Ni(OAc)_2$ solution was replaced with 0.9% NaCl through Sephadex G-50 column to obtain blank LP. Similarly, the extraliposomal $Ni(OAc)_2$ solution was replaced with 300 mM NaCl solution containing 20 mM HEPES through Sephadex G-50 column, thus a Ni^{II}-ion gradient was obtained between the internal and the external aqueous phase of LP. To load As^{III} into LP (AsLP), 20 mM of As^{III} solution was added into the external aqueous phase of LP under a stir at 400 rpm and 60 °C for 30 min, and then the extra As^{III} was removed by Sephadex G-50 column using above NaCl/HEPES solution as an eluting buffer.

Tf-modified AsLP was prepared by post-insertion method. Tf-PEG2000-DSPE was synthesized (referring to supplementary information), and then stirred at 400 rpm and 55 °C with the blank LP for 30 min (Tf/lipids = 1/500, molar ratio), the Tf-LP was obtained by passing through Sepharose CL-6B column using 0.9% NaCl as the eluting buffer. Then, As^{III}-loaded Tf-LP (Tf-AsLP) was acquired according to the above As^{III} loading method.

2.3. *Characterizations of liposomes*

The prepared AsLP and Tf-AsLP were diluted in deionized water. Zetasizer Nano ZS90 (Malvern, UK) was applied to measure particle Z-average size and ζ-potential [15,16]. Morphology was observed under a 200 kV cryo-EM microscope (Tecnai G2 F20, FEI, US).

The As^{III} content in LP was determined by AFS-8230 Atomic Fluorescence Spectrometer at 193.7 nm (AFS, Jitian, Beijing, China). 10 μl AsLP or Tf-AsLP after treated with a Sephadex G-50 column was firstly dissolved in 3 ml methanol/chloroform (1/4, v/v), 5% HCl (1 ml) was added to mix with the organic solution for about 3 min. After centrifuged for 5 min at 500 g, the concentration of As^{III} in supernatant to be determined was diluted with 1% thiourea in 5% HCl. The encapsulation efficiency (EE) and drug loading (DL) were calculated as in Eqs. (1) and (2).

$$EE\ (\%) = \frac{m_{AsIII\ in\ liposomes}}{m_{addition\ of\ AsIII}} \times 100\% \quad (1)$$

$$DL\ (\%) = \frac{m_{AsIII\ in\ liposomes}}{m_{AsIII\ in\ liposomes} + m_{lipids\ after\ column}} \times 100\% \quad (2)$$

The Tf modification on liposomes was detected by Bradford protein assay kit (Meilun, Dalian, China) [17]. 10 μl Tf-AsLP after treated with a Sephadex G-50 column was firstly dissolved in 3 ml chloroform, and then 1 ml deionized water was mixed with the organic solution with 3-min vortex (08-3G, Meiyingpu Instrument Manufacturing Co., Ltd, Shanghai). 10 μl the supernatant fluid was added into a 96-well plate and incubated with Coomassie brilliant blue G-250 for 5 min then detected by a microplate reader (Synergy HTX, BioTek) at 595 nm. Tf amount was calculated as in Eq. (3).

$$Tf\ (\%) = \frac{m_{Tf\ in\ Tf-LP}}{m_{Tf-LP}} \times 100\% \quad (3)$$

2.4. *Stability of liposomes*

The stability of Tf-AsLP and AsLP was evaluated in simulated physiological conditions. The particle size distribution and ζ-potential in pH 4.5, 5.0 and 7.4 phosphate buffer solutions (PBS) or 10% fetal bovine serum (FBS, v/v) were measured for 24, 48 and 72 h at 37 °C.

2.5. *Evaluation of in vitro AsIII release characteristics*

In vitro release profiles were measured in pH 4.5, 5.0, 6.0 and 7.4 PBS, respectively. Briefly, 0.5 ml AsLP, Tf-AsLP or As^{III} solution were added into different dialysis bag (MWCO = 14,000 kDa, size: 2.5 cm×3.5 cm). The dialysis bag was placed into 70 ml different buffers to meet the sink condition and stirred at 120 rpm, 37 °C. 4 ml the medium was taken out for the determination at different time point, and 4 ml fresh buffer solution was added to the external fluid.

2.6. *Cellular experiments*

2.6.1. *Cell lines and primary leukemia samples*

HL-60 cells were purchased from Shanghai Institute of Biochemistry and Cell Biology. K562 cells (human chronic myeloid leukemia), THP-1 cells (human acute monocytic leukemia) were purchased from Procell Life Science & Technology Co., Ltd. (Wuhan, China). HL-60 cells and K562 cells were respectively cultured in IMDM supplemented with 20% and 10% (v/v) FBS with 1% (v/v) penicillin-streptomycin (P/S). THP-1 cells were cultured in RPMI with 10% (v/v) FBS and 0.05 mM β-mercaptoethanol (with 1% P/S). All cells were cultured in a humid atmosphere of 5% CO_2 at 37 °C.

Human primary leukemia peripheral blood or BM samples were provided by the Hematology and Oncology Department of Shanghai Pudong Hospital. The study (QWJWXM-03) was approved by the ethical review committee of Shanghai Pudong Hospital. The smears of the collected samples were stained with Wright's staining solution. Then, Percoll cell separation reagent was employed to extract leukocytes from the primary

samples by density gradient centrifugation at 400 g for 25 min. The corresponding bands were drawn, and cultured with IMDM containing 20% FBS. The remaining cells were resuspended in Cryopreservation solution (Cyagen, US), stored in liquid nitrogen.

2.6.2. Cellular uptake and intracellular location in HL-60

To evaluate the specific uptake mediated by Tf, coumarin 6 (Cou-6) labelled LP and Tf-LP were prepared (referring to supplementary information). CytoFlex S Flow cytometry (FCM, Beckman, Shanghai) and inverted fluorescence microscope were successively applied to the detection of fluorescence expression. HL-60 cells (1×10^6 per well) were suspended in 0.5 ml serum-free medium and seeded in a 24-well plate, then Cou-6, Cou6-labeled LP and Tf-LP were added at Cou-6 concentration of 0.3 μg/ml. To evaluate the specificity of uptake, 200 μg/ml Tf were additionally incubated with HL-60 cells for 30 min prior to Tf-LP. The cells were washed and analyzed by FCM after incubation for 2 h. For imaging, the cells after incubation were removed to a new 24-well plate which was pre-saturated with 10 μg/ml PLL for further 15 min incubation. The adherent HL-60 cells were washed with PBS twice and visualized by inverted fluorescence microscope (DMI4000D, Leica, Germany).

In order to confirm whether Tf-modified LP were selectively captured by leukemia cells in circulatory system, the peripheral blood from NOD/SCID mice was extracted and mixed with HL-60 cells, so that the concentration of HL-60 cells in blood reached 10×10^9/l, which was the diagnostic criteria of promyelocytes in peripheral blood of non-high-risk APL patients [18,19]. Then, Cou-6 labeled LP were incubated with the blood sample at 37 °C for 60 min, and all leukocytes were collected by lysis of RBC and stained with PE anti-human CD45. HL-60 cells were distinguished from murine PWBC by FCM. The mean fluorescence of Cou-6 in HL-60 cells and murine PWBC were applied to evaluate the uptake of Tf-modified LP.

After that, the uptake of AsLP and Tf-AsLP was quantified. HL-60 cells (1×10^6 per well) were treated with AsLP and Tf-AsLP at a drug dose of 25 μM. After incubated for 0, 2, 4, 6, 8, 12, 24, 72 and 120 h, the cells were collected, washed and suspended in 1 ml PBS, respectively. 400 μl the cell suspension was centrifugated, discarded all the supernatant, added 50 μl lysate to resuspend the precipitated cells in ice bath for 15 min. The solution was used to measure the total protein by Bradford kit. Another 400 μl of the cell suspension was centrifugated, discarded all the supernatant. The cells were resuspended with 500 μl nitric acid for 48 h to lyse HL-60 cells. Then, the samples were diluted with deionized water and analyzed by AFS at 193.7 nm.

To observe the intracellular distribution of liposomes, HL-60 cells (1×10^6 per well) were suspended in 0.5 mL serum-free medium. The cells were firstly incubated with Cou6-LP or Tf-Cou6-LP and further treated with LysoTracker Red for another 30 min at 37 °C. Cells were transferred to PLL pre-saturated confocal dish for 10 min after incubation. The adherent HL-60 cells were washed with PBS and fixed with 4% paraformaldehyde for 15 min. The distribution of cells was examined by confocal laser scanning microscopy (CLSM, SP8, Leica, Germany) (λex = 577 nm and λem = 590 nm).

2.6.3. In vitro cytotoxicity

HL-60, K562, or THP-1 cells were respectively seeded in 96-well plates at 1×10^4 per well, and incubated with free As^{III}, LP, AsLP and Tf-AsLP for 72 h at 37 °C. Ten μl CCK-8 was added into medium and incubation for about 4 h. Microplate reader (Synergy Neo2, BioTek, America) was used to measure the absorbance at 450 nm and 630 nm.

2.6.4. In vitro cell apoptosis

HL-60 cells were seeded in 24-well plate at 1×10^6 per well and incubated with free As^{III}, LP, AsLP and Tf-AsLP for 72 h. Then cells were washed by PBS for 3 times and collected through centrifugation at 300 g for 2 min. Subsequently, cells were redispersed and stained with Annexin V-FITC/PI kit for 30 min at room temperature. Then FCM was applied to detected the apoptosis of cells. The apoptosis of THP-1, K562 or primary leukemia cells from clinic patients at the dose of 25 μM As^{III} were detected by the same method.

Similarly, primary leukemia cells were seeded at 1×10^6 per well and incubated with free As^{III}, LP, AsLP and Tf-AsLP for 72 h. After washed by PBS and stained with Annexin V-FITC/PI kit, the apoptosis of cells was detected by FCM.

2.6.5. Reactive oxygen species (ROS) level

For ROS examination, 1×10^6 per well HL-60 cells were seeded in 24-well plate. After treatment with free As^{III}, LP, AsLP and Tf-AsLP for 12 h at the concentration of 25 μM, cells were washed with PBS and stained with DCFH-DA probe (Meilun, Dalian, China) at 37 °C for 30 min. Then cells were washed 3 times with serum-free medium and analyzed by FCM.

2.6.6. Caspase-3 activity

HL-60 cells were seeded at 1×10^6 per well in a 24-well plate. After 12 h treatment of blank LP, free As^{III}, AsLP and Tf-AsLP (at a drug dose of 25 μM), HL-60 cells were washed for three times and suspended in the cell lysates for 15 min in ice bath followed by centrifugation at 16,000-20,000 g for 15 min. The supernatant was stored at – 80 °C for detection.

The total protein of the supernatant was measured by Bradford assay method, and tested by Caspase-3 activity kit. Firstly, the supernatant was diluted to a protein concentration of 1 mg/ml. According to the procedure, 50 μl diluted sample were mixed with 40 μl detection solution and 10 μl Ac-DEVD-pNA (2 mM), then incubated at 37 °C for 60 min. The absorbance was measured at 405 nm through Microplate reader.

2.6.7. Cell differentiation

Cell differentiation was detected by FCM. HL-60 cells were seeded at 1×10^6 per well in a 24-well plate. After the treatment of free As^{III}, LP, AsLP and Tf-AsLP for 5 d, the cells were washed with PBS and stained with APC-labeled anti-human CD11b for 30 min at room temperature, and analyzed by FCM.

2.7. Animal experiments

All animal experiments in present study were conducted in compliance with the guidelines of the Ethics Committee of Animal Center of Fudan University (No. 2018-11-YJ-JYY-01, 2018-11-YJ-JYY-02).

Table 1 – Properties of liposome in pH 7.4 PBS. ($n = 3$).

LPs	Z-average Size (nm)	PDI	ζ-potential (mV)	DL (%)	EE (%)
LP	108.20 ± 0.98	0.17 ± 0.015	–6.55 ± 0.18	/	/
Tf-LP	125.63 ± 2.23	0.13 ± 0.012	–8.59 ± 0.90	/	/
AsLP	114.80 ± 1.56	0.17 ± 0.044	–7.87 ± 0.21	1.86 ± 0.12	90.23 ± 1.88
Tf-AsLP	128.22 ± 1.40	0.15 ± 0.011	–10.48 ± 1.01	2.44 ± 0.04	82.94 ± 2.41
Tf-RALP	116.23 ± 2.03	0.18 ± 0.023	–9.90 ± 2.01	2.04 ± 0.07	90.54 ± 4.05

PDI: polydispersity index, DL: drug loading, EE: encapsulation efficiency.

2.7.1. *Pharmacokinetic evaluation in rats*

Pharmacokinetic study was performed in SD rats. SD rats (240-250g) were purchased from Shanghai Slac Laboratory Co., Ltd. Nine rats were randomly divided into 3 groups and administered intravenously of free As^{III}, AsLP or Tf-AsLP at the dose of 0.75 mg/kg As^{III}. About 0.5 ml blood was collected at 0, 5, 15, 30, 60, 120, 240, 480, 720, 1,440, 2,880 and 4,320 min and stored in centrifuge tubes containing heparin sodium.

For As^{III} determination in blood, 0.2 ml blood and 9.8 ml nitric acid were added into polytetrafluoroethylene (PTFE) tank, then digested using MDs-10 microwave digestion system (Xinyi, Shanghai, China) at the procedure as follows: 0-20 min, 25- 150 °C; 20-30 min, 150-180 °C; 30-60 min, 180-25 °C. The solution was collected and diluted to 10 mL with deionized water. The samples were further diluted 10 times with 1% thiourea in 5% HCl, and determined by Generation-AFS. The regression equation was A = 100.7C-11.135, r = 0.9999, and the detection limit was 0.05 μg/l. The parameters were calculated by DAS 2.0.

2.7.2. *In vivo efficacy and safety on subcutaneous tumor of HL-60 cells*

18-22 g Male nude mice were purchased from the Shanghai Slac Laboratory Co., Ltd. To establish an initial subcutaneous model, HL-60 cells (1×10^7/ml) were suspended in matrigel/PBS (1:1, v/v) solution. And nude mice were subcutaneously injected 200 μl cell suspension into the right flank. After 2 weeks, tumor tissue was homogenized into a single-cell suspension. After stained with PE-labeled anti human CD45 and tested by FCM, HL-60 cells accounted for 84% of the suspension, indicating the xenografted tumor model was established successfully. The cell suspension was filtered through 70 mm cell sieve to move connective tissue and washed with PBS to obtain APL cells. A secondary transplanted xenografted model was established by injecting subcutaneously the extracted APL cells under the right armpit of nude mice. The mice were selected to evaluate the *in vivo* anti-leukemia efficacy when tumor size around 80 mm^3.

For preliminarily evaluating the effect of AsLP and Tf-AsLP, the mice were randomized into 4 treatment groups ($n = 6$) and administered intravenously with free As^{III}, AsLP and Tf-AsLP at a dose of 0.5 mg/kg As^{III} every 3 d for 5 times in total. Then, RA-loaded liposomes were prepared (referring to supplementary information). For studying the synergism effect with liposomal As^{III} and liposomal RA, sequential administration (Tf-RALP → Tf-AsLP), and co-administration (Tf-AsLP + Tf-RALP) were set up. Sequential administration (Tf-RALP → Tf-AsLP): Firstly, Tf-RALP was administrated 2 times at a dose of 1.5 mg/kg RA, followed by 3 times Tf-AsLP at a dose of 0.5 mg/kg As^{III}. Co-administration (Tf-AsLP + Tf-RALP): Tf-AsLP and Tf-RALP were administered together every 3 d for 5 times at a dose of 0.5 mg/kg As^{III} and 1.5 mg/kg RA. The mice were randomized ($n = 6$), tumor volume and body weight were monitored throughout the study. The tumor mass was homogenized and filtered through 70 mm cell sieve to obtain APL cells, then cells were stained with APC labeled anti-human CD11b and detected by FCM. After 15 d of treatment, tumor-bearing mice were sacrificed to collect tissues and organs for H&E analysis. A death event was recorded and the mouse were euthanized when any of the following occurs: individual tumor volume reached 2,000 mm^3 or any length reached 2 cm or body weight loss over 20% or when mice became moribund.

2.7.3. *Effect on orthotopic model of leukemia mice*

NOD/SCIDmice obtained from Shanghai Slac Laboratory Co., Ltd. were used to establish orthotopic leukemia model. The NOD/SCID mice were firstly irradiated with ^{60}Co at a dose of 2 Gy. After 24 h, 4×10^6 HL-60 cells were injected through the tail vein and raised for 3 to 4 weeks [20]. Every 7 d, 50 μl blood was taken from the orbit of mice, and stained with 2.5 μl APC labeled anti-human CD45. The proportion of HL-60 cells in the peripheral blood of mice was measured by FCM. After the model mouse was sacrificed, the outer skin was disinfected with 75% alcohol, the femur of the hind leg was taken, and the BM cavity was repeatedly washed with PBS to collect BM cells. BM cells were made into smears and observed under the microscope. When a significant increase of HL-60 in both blood and BM was observed, the APL orthotopic model was established successfully.

APL NOD/SCID mice were weighed, randomized into 4 groups ($n = 7$) and administered intravenously with different preparations at a dose of 0.5 mg/kg As or 1.5 mg/kg RA every 3 d for 4 times. The body weight and survival rate were monitored throughout the study. After the administration, blood was taken from the orbit of NOD/SCID mice and added to the EDTA anticoagulation tube. The blood was examined by a Mindray animal blood cell analyzer (Shenzhen, China), with an injection volume of 100 μl. BM samples were taken from mice, and 5 μl APC labeled anti-human CD11b or PE labeled anti-human CD45 was added to every 100 μl samples and stained at room temperature for 30 min. The proportion of positive cells was detected by FCM.

After the administration, blood was taken from the orbit of NOD/SCID mice, and after left at 4 °C for about 1 h. Alanine aminotransferase (ALT), Alkaline phosphatase

(ALP), Creatinine assay kits were used to detect biochemical indicators in serum by automatic biochemical analyzer (Dulei, Shenzhen, China). For histopathology analysis, the organs of NOD/SCID mice including heart, liver, spleen, lung, spleen were harvested and stored in 4% formaldehyde. The organs were stained with H&E and observed under the microscope. DAPI, CD45 antibody and CD11b antibody were applied to stain the liver and spleen of the mice to examine the infiltration of leukemia cells in tissues, and the slices were photographed by CLSM.

2.8. Statistical analysis

The data were presented as mean ± standard deviation (SD). t-test was applied to determine significant differences by GraphPad Prism 6 (CA, USA). In all analyses, the statistical significance was considered as $^{*}P < 0.05$, $^{**}P < 0.01$, $^{***}P < 0.001$.

3. Results and discussion

3.1. Characterization of liposomal [AsIII, NiII] complex with acid-triggered release

Here, a Ni-ion gradient method was used to load arsenite into liposomes, Tf-PEG2000-DSPE was synthesized by the reaction between DSPE-PEG2000-COOH and Tf-NH_2 using Sulfo-NHS/EDC method (Fig. S1) to prepare Tf-modified liposomes through post-inserting Tf-PEG2000-DSPE in preformed liposomes. The content of Tf in the prepared liposomes was accounted for about 2.34% of the total lipid (w/w). The particle Z-average sizes and ζ-potentials of different prescriptions were listed in Table 1. All the LP were slightly negatively charged and the Z-average sizes were in the range of 100-130 nm. Among them, Tf modification slightly increased the size of Tf-LP. EE and DL of As^{III} in two liposomes were over 80% and around 2%, respectively. The Cryo-EM images showed that the morphology of AsLP and Tf-AsLP was nearly spherical (Fig. 1A & 1B).

The stability of liposomal [As^{III}, Ni^{II}] complexes was investigated in different biological mimicking conditions. As shown in Fig. 1C, the zeta potentials of AsLP and Tf-AsLP were basically unchanged in three pH media within 72 h. The particle sizes and PDI of two liposomes in different media were relatively stable within 72 h due to a high phase transition temperature of DSPC (55 °C) in formulation, though the curves displayed slight fluctuations (Fig. 1D & 1E). Moreover, the size curves of Tf-modified AsLP showed smaller fluctuation as compared with those of unmodified AsLP, especially in serum-containing PBS, implying that the plasma protein binding of Tf-AsLP in peripheral blood would be negligible.

The tests of *in vitro* release were carried out in different pH buffers. As shown in Fig. 1F&1G, the free As^{III} completely spread out of the dialysis bag in 2 h, in contrast, the release profiles of both AsLP and Tf-AsLP obviously displayed the sustained and acid-sensitive release properties. At 72 h, the As^{III} release percentages from two LP were about 19%, 25% and 30% in pH 7.4, 6.0 and 5.0 buffer, respectively, while that was over 63% in pH 4.5 buffer. The significant acid-triggered release characteristic of the liposomal arsenic-nickel complex is identical with previous reports [21]. It could be reasonably predicted that the As^{III}-loaded LP would be relatively stable at normal physiological pH, but arsenic could be easily released once LP were internalized into the intracellular acidic environment. The mechanism of As^{III} loading was shown in Fig. 1H, the concentration gradient of $Ni(OAc)_2$ solution was firstly formed for effective As^{III} loading, and then the $HAsO_2$ in the external phase actively came across the lipid membranes and formed insoluble $Ni(AsO_2)_2$ accumulated in the internal aqueous phase of LP, which was mainly responsible for the acid-sensitive drug release.

3.2. Biological functions of Tf-AsLP

3.2.1. *In vivo* long-circulation function

The circulation time of As-loaded liposome in blood was evaluated on SD rats. the results were shown in Fig. S2 and Table 2. After intravenous administration of the same dose of As^{III}, the pharmacokinetic curves of liposomal As^{III} exhibited significant difference with that of free As^{III}. Free As^{III} was rapidly cleared, with the shortest $T_{1/2}$ and the lowest AUC. In contrast, the circulating time of AsLP and Tf-AsLP was significantly prolonged, and the PK curves of two liposomes had almost the same change trend. As compared to free As^{III}, the $T_{1/2}$ of AsLP and Tf-AsLP was increased by about 64 and 88 folds, respectively, both $MRT_{0\text{-}t}$ was over 7 times longer, and AUC was increased by 8 times. Moreover, Tf-AsLP displayed a slightly longer retention time than AsLP group. The above results suggested that Tf-AsLP could prolong the *in vivo* circulation time of As^{III}, maintain a stable As^{III} concentration in blood over 72 h.

In the process of delivery, the As^{III} level in blood was the key factor determining efficacy or toxicity. Compared with free As^{III}, AsLP and Tf-AsLP showed longer circulation in blood within a certain period of time. Combined with the characteristics of acid-sensitive release, we inferred that drug release of LP in neutral fluids was relatively low, which was conducive to improve the safety after entered the body.

3.2.2. *CD71-mediated specific recognition of leukemia cells*

The expression of CD71 on HL-60 cells (APL), THP-1 cells (AML), and K562 cells (CML) was first confirmed by FCM (referring to supplementary methods). As depicted in Fig. S3, there were 82% of HL-60 cells, 67% of K562 cells, and 88% of THP-1 cells to express CD71, respectively, indicating that most of cells for three leukemia cell lines possess Tf receptors. Moreover, HL-60 cells showed the highest level of CD71 expression as compared with THP-1 cells and K562 cells.

To verify the cell-specific binding, cellular uptake of Cou-6 labeled LP and Tf-LP was detected in HL-60 cells via inverted fluorescence microscope (DMI4000D, Leica, German) and FCM. The fluorescence intensity of cells (Fig. 2A) treated by Tf-LP was markedly higher than that of cells treated by LP, while the cellular fluorescence of Tf pre-incubated cells prior to Tf-LP treatment was reduced. The similar phenomena were also found in the FCM experiment (Fig. 2B and S4A), Tf modification could significantly improve the cellular uptake of LP, the mean fluorescence of Tf-LP was 1.8 times higher than that

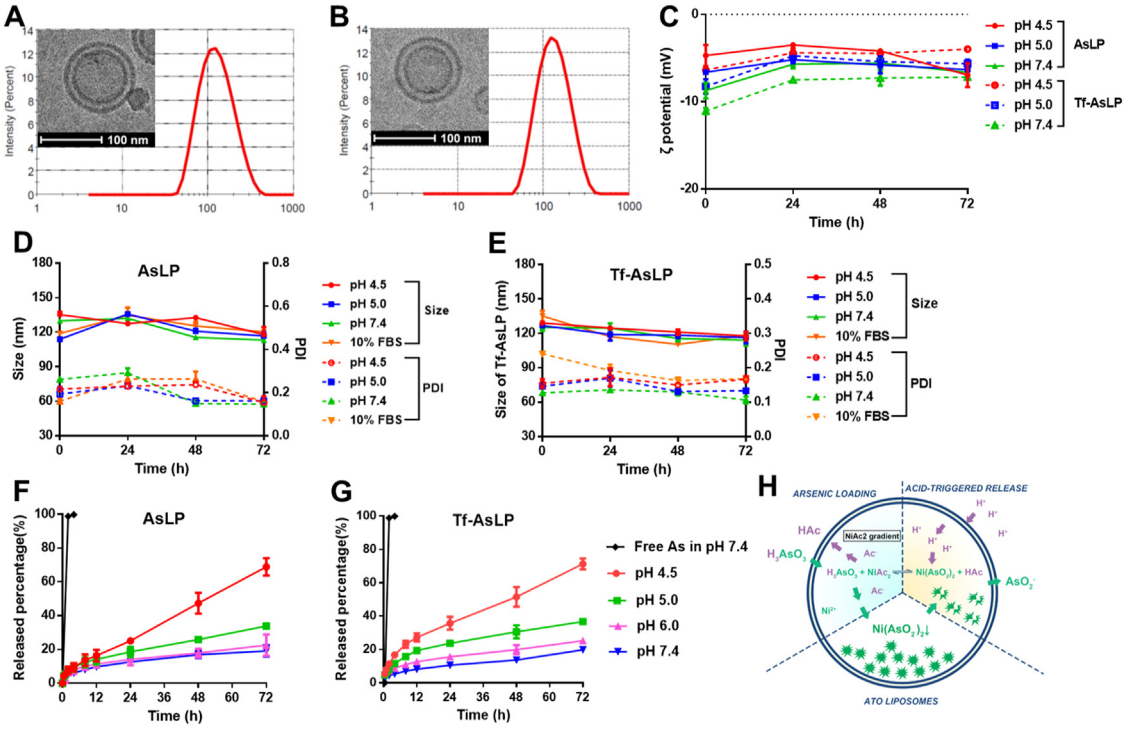

Fig. 1 – Characterization of AsLP and Tf-AsLP. The size and Cryo-EM images of AsLP (A) and Tf-AsLP (B). Effect of different buffer solutions on zeta potential (C), particle size and PDI of AsLP (D) and Tf-AsLP (E) was measured using a Zeta sizer Nano ZS. *In vitro* drug release of AsLP (F) and Tf-AsLP (G) in different PBS buffers at 37 °C. The As loading and acid-sensitive release were showed in (H) according to the relevant literature [21]. Data was presented as mean ± SD. (n = 3).

Table 2 – Pharmacokinetic parameters of free As^{III} and LPs. (n = 3).

Parameters	Free As^{III}	AsLP	Tf-AsLP
C_{max} (mg/l)	6.09 ± 0.58	7.93 ± 0.67 *	8.37 ± 0.26 *
$T_{1/2}$ (h)	0.04 ± 0.01	2.57 ± 1.72 ***	3.51 ± 3.70 ***
MRT_{0-t} (h)	4.60 ± 0.02	32.78 ± 0.62 ***	34.61 ± 1.33 ***
AUC_{0-t} (mg/l·h)	28.82 ± 2.89	226.74 ± 7.03 ***	247.20 ± 20.50 ***

Statistical comparison of free As and LP. (*$P < 0.05$, **$P < 0.01$, ***$P < 0.001$).

of unmodified ones ($P < 0.001$). Furthermore, HL-60 cells were pre-incubated with 200 μg/ml Tf followed by Tf-LP. A reduction of 22.6% was observed in CD71-saturated cells by FCM. Since the uptake of Cou-6 labeled LP could not completely represent that of As^{III}-encapsulated LP due to the different location of Cou-6 (in the bilayer) and arsenic-nickel complex (in the inner water phase) in liposomes, the internalized amounts of AsLP and Tf-AsLP were determined by AFS analysis. The As^{III} amount of Tf-AsLP in cells was always higher than that of AsLP, and the uptake difference between two LP gradually increased with the extension of incubation time, it was more than 2 times after 120 h (Fig. 2C). These results confirmed that Tf-modified liposomes could increase the cellular uptake via CD71-mediated specific binding.

Additionally, the liposomes uptake by leukocyte in the circulatory system of leukemia mice was simulated *in vitro* by the co-incubation of Cou-6 labeled liposomes and the mixture of HL-60 cells and the peripheral blood from a healthy volunteer. As shown in Fig. 2D and S4B, *the* mean fluorescence of two LP in HL-60 cells was over 4.5 times higher than in normal PWBC, among them, the uptake of Tf-modified LP by HL-60 was conspicuously higher than that of the unmodified LP, but no statistical difference in normal PWBC. In addition, the peripheral blood was directly incubated with Cou-6 labeled LP, the leukocytes were collected and detected by FCM to quantify the uptake of different PWBC in blood. For lymphocytes, monocytes and granulocytes, the uptake difference between LP and Tf-LP was not found, indicating that CD71 was not overexpressed in normal PWBC (Fig. S5A& S5B). The effects of free As^{III} and its liposomes on erythrocytes were evaluated by quantifying arsenic in RBC (Fig. S5C). It was found that there was no obvious accumulation of As^{III} in the RBC for both free As^{III} and two As^{III}-loaded LP groups, one possible reason could be that the erythrocyte membrane is semi-permeable for As^{III} and its liposomes leading to the blocking of transmembrane transport expect water. Thus, it could be predicted that the toxicity of the present Tf-AsLP and AsLP would be quite low for both normal leukocytes and

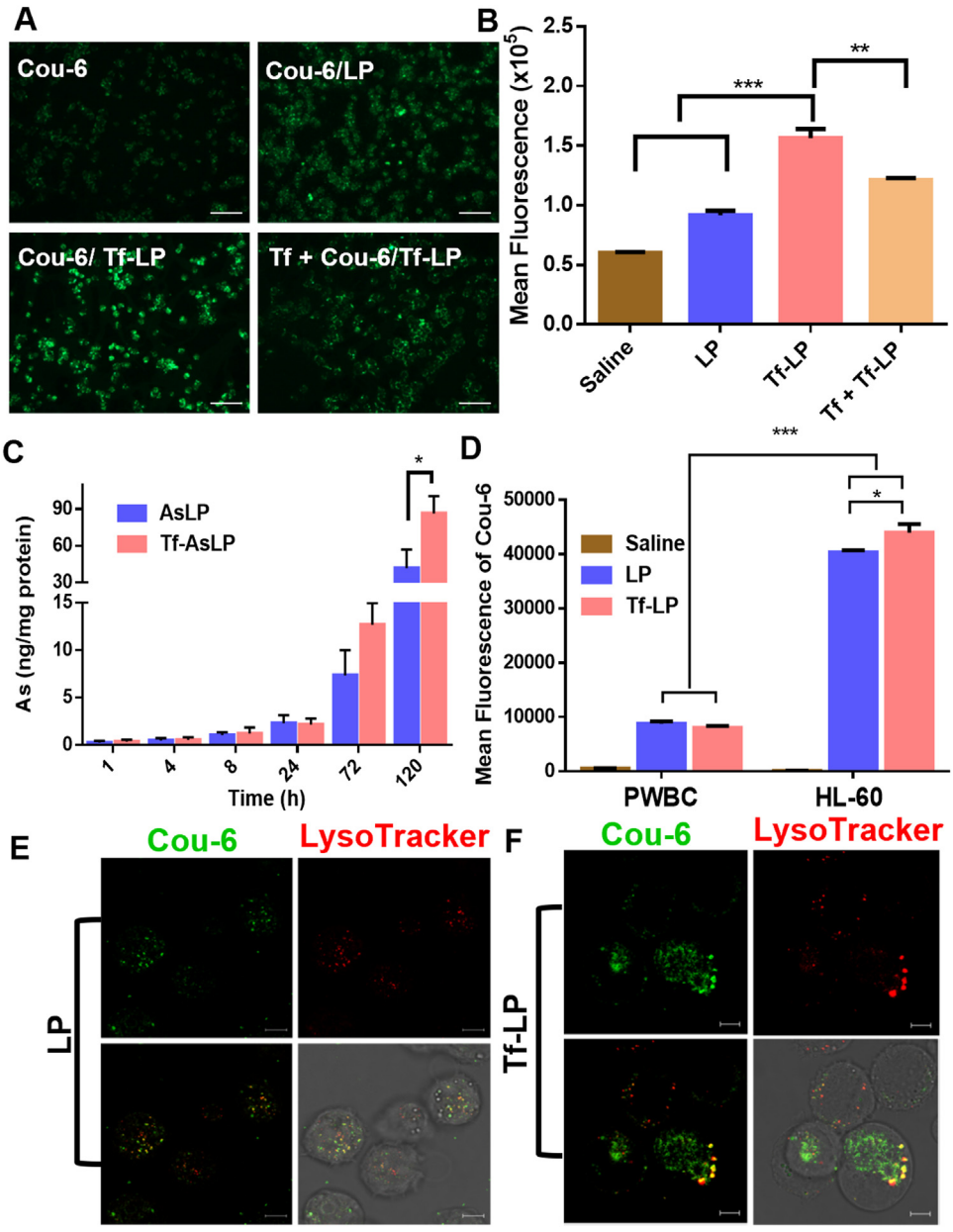

Fig. 2 – *In vitro* cellular uptake on HL-60 cells. Cellular uptake of Cou-6 labeled LPs investigated by inverted fluorescence microscope (A) (Bar: 100μm), flow cytometry in HL-60 cells (B) and in the mixture of HL-60 cells and murine peripheral blood (D). The uptake of As-loaded LP by HL-60 cells were quantified by AFS analysis (C). ($n = 3$, *$P < 0.05$, **$P < 0.01$, ***$P < 0.001$). Intracellular distribution of Cou6-labeled LP (E) and Tf-LP (F) in HL-60 cells imaged by CLSM. LysoTracker was used to label lysosomes with red fluorescence, Cou-6 was showed in green fluorescence, and the merged signal was judged by yellow fluorescence. (Bar: 3 μm).

erythrocyte once in the blood circulation system owing to the low uptake of normal blood cells.

The intracellular distribution of the prepared LP in HL-60 cells was following observed by CLSM (Fig. 2E&2F). After incubation of HL-60 cells and Cou-6 labeled LP or Tf-LP, green-fluorescent Cou-6 was observed in the cytoplasm, and the intensity of Tf-LP was significantly stronger than that of LP. Moreover, the significant yellow fluorescence was displayed in two LP groups due to the colocalization of green Cou-6 and red lysosomes, especially Tf-LP with a higher fluorescence intensity in lysosomes. The above results suggested that As-loaded LP could be efficiently endocytosed by APL cells in blood, and more arsenic-nickel complexes in Tf-LP would be transported into the lysosome via CD71-mediated specific uptake, leading to more As^{III} release from liposomes in acidic environment of the lysosome.

3.3. *Tf-AsLP induced cell apoptosis and differentiation*

CCK-8 assay was applied to evaluate the cytotoxicity. HL-60, K562 and THP-1 cells were incubated with blank LP, free As^{III}, AsLP or Tf-AsLP at various concentration gradients for 72 h. As

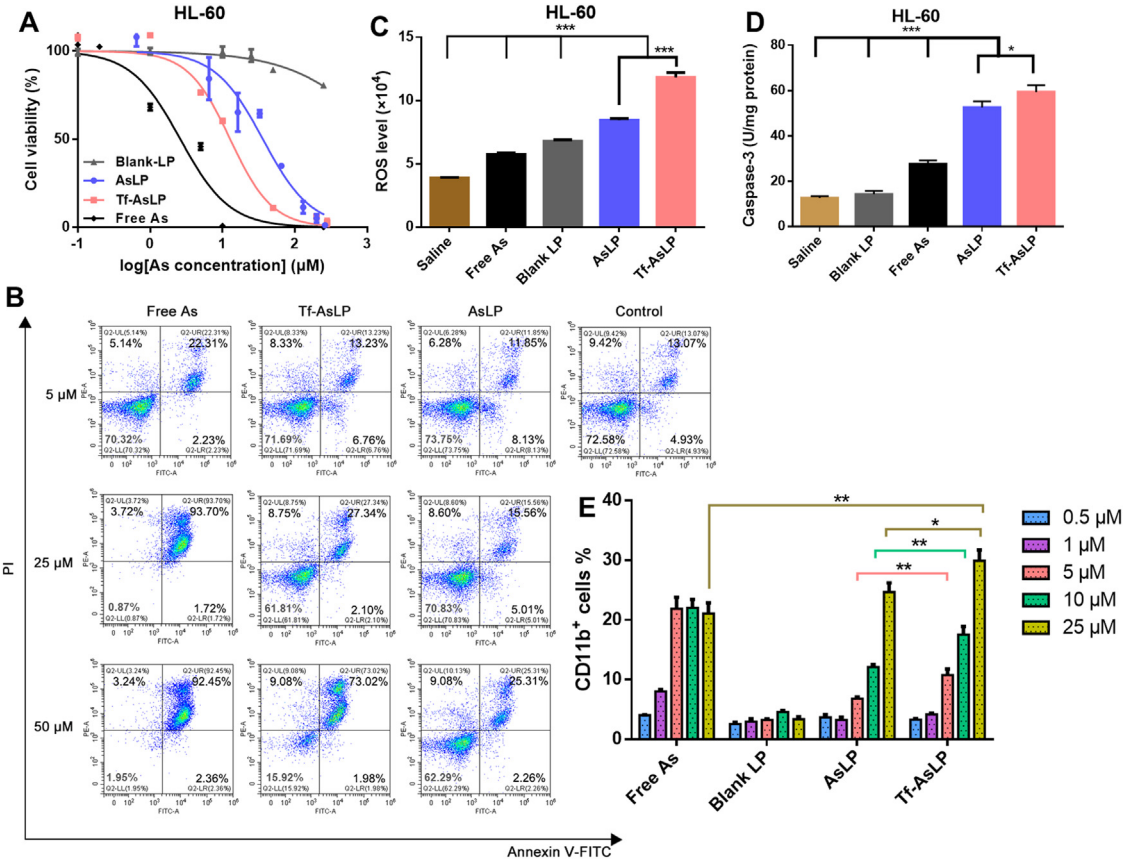

Fig. 3 – Cytotoxicity, apoptosis and differentiation on HL-60 cells. Cytotoxicity of free As or liposomes (A) was assessed by CCK-8 assay at 37 °C for 72 h. Cell apoptosis rate was determined by Annexin V-FITC/PI staining (B), the lower-left, upper-left, lower-right and upper-right quadrants represented the viable, dead, early apoptotic and late apoptotic cells, respectively. ROS level (C) and Caspase-3 activity (D) were detected by DCFH-DA probe and Caspase-3 kits. Cell differentiation of HL-60 cells induced by free As or LPs quantified by flow cytometry, the blank group referred to the blank LP with the same phospholipid concentration as the drug-loaded LP (E) ($n = 3$, *$P < 0.05$, **$P < 0.01$, ***$P < 0.001$).

Table 3 – IC50 of free As^{III} and different As^{III} loaded LPs. (μM, $n = 3$).

Cell lines	Free As^{III}	AsLP	Tf-AsLP
HL-60	2.62	36.21	13.43
K562	3.06	10.38	7.37
THP-1	2.41	42.71	8.94

shown in Fig. 3A and S6A&S6B, the blank LP had a negligible cytotoxicity to three types of cells. As compared with AsLP and Tf-AsLP, free As^{III} exhibited the strongest cytotoxicity due to the direct interaction with cells. IC50 values were listed in Table 3. For two AsLP, the IC50 value of AsLP was 2.7 times (HL-60), 4.8 times (THP-1) and 1.4 times (K562) higher than those of Tf-AsLP, respectively, and the cytotoxicity of Tf-AsLP was conspicuously higher than that of AsLP for all three leukemia cell lines, suggesting that Tf-modified AsLP possessed a credible effect on inhibiting the growth of APL cell line and other leukemia cell lines.

The apoptosis used to evaluate *in vitro* efficacy was a key index for the programmed death. Cells in different apoptotic stages were stained with Annexin V-FITC/PI kit and analyzed by FCM. The apoptosis rate of HL-60 cells induced by different administration groups was ranked as follows: free As^{III} > Tf-AsLP > AsLP, and it increased with the increase of the arsenic concentration (Fig. 3B). The phenomenon was also found in either K562 or THP-1 cell line as shown in Fig. S6C. The mechanism of AsLP promoting apoptosis was investigated by detecting the ROS level and Caspase-3 activity of APL cells (Fig. 3C&3D). DCFH-DA probe was applied to determine the intracellular ROS level. DCFH was generated by hydrolysis of DCFH-da with esterase in HL-60 cells, and then oxidized to generate DCH, revealing fluorescent signal for analyze. Both blank LP and free As^{III} exhibited significantly lower ROS levels than As-loaded LP, because blank LP are almost no effect on cell viability, but 25 μM of free As^{III} with a strong cytotoxicity causes high cell mortality rate and low viability of living cells. In contrast, Tf-AsLP showed the strongest ROS induction ability, which was 1.4 times higher than that of AsLP. Similarly, the Caspase-3 level treated with saline or blank LP was the lowest (about 12-14 U/mg protein) among all treatment groups. For arsenic treatment groups, the AsLP group as well as the Tf-AsLP group resulted in about 3 folds increase in the Caspase-3 activity than free As^{III}, whereas the

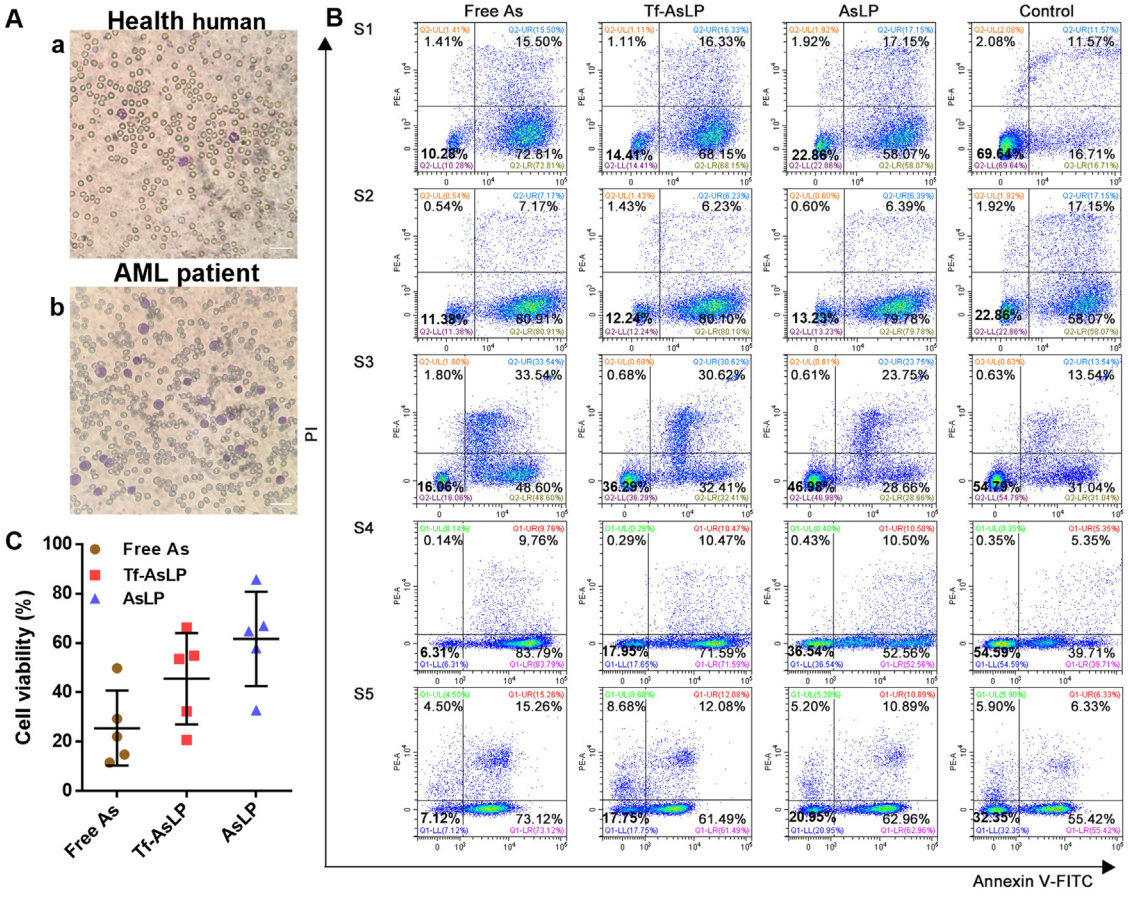

Fig. 4 – (A) Smears of peripherical blood from health human (a) and AML patient (b) taken by microscope (Bar: 25μm). Cell apoptosis of primary leukemic samples determined by Annexin V-FITC/PI kit. (B) The lower-left, upper-left, lower-right and upper-right quadrants represented the viable, dead, early apoptotic and late apoptotic cells. (C) The percentage of cell viability was calculated by the lower-left datum of drug group divided by that of control group.

activity in Tf-AsLP group was significantly higher than AsLP group ($P < 0.05$). It can be inferred from Fig. 3C&3D that Tf-AsLP possessed the strongest effect of inducing apoptosis in APL cells by increasing the ROS level and enhancing the Caspase-3 activity. As^{III} was reported to represent an apoptosis-inducing agent through phosphatidylserine externalization, caspase 3 activation and nucleosomal DNA fragmentation [22]. Combined with the results of viability of LP on cells, it could be found that As^{III} loaded LP induced HL-60 to produce a higher level of ROS after Tf modification. Through the activation of p53 tumor suppressor gene, the activity of Caspase-3 enzyme in the cells was significantly improved, and finally more HL-60 cells were induced to apoptosis.

In order to explore the clinical applicability of the present Tf-AsLP, five clinical leukemia samples from patients in Shanghai Pudong Hospital were collected randomly (Table S1). Firstly, Wright's stained smears were prepared and imaged in Fig. 4A. The RBC in normal blood showed thick in the edge and sunken in the middle, no nucleus and organelle were observed, the PWBC were stained as purple, nucleated and reasonably distributed (Fig. 4Aa). However, the peripheral blood from leukemia patients distributed a lot of leukemia cells (Fig. 4Ab). Then, Annexin V-FITC/PI kit was applied to detect primary cells at different apoptotic stages and analyzed using FCM. In the period of culturing primary cells *in vitro*, as the increase of times, serious aging occurred, leading to a certain proportion of apoptotic cells in control group without drug treatment. Thus, after treatment with free As^{III} or As-loaded LP, the ratio of the number of viable cells after administration to the number of viable cells in the control group was used to analyze the apoptosis of primary cells. As shown in Fig. 4B&4C, primary leukemia cells displayed different degrees of apoptosis. The cell survival rate of each group was listed as: Free As^{III} < Tf-AsLP < AsLP, the trend was identical with that of HL-60 cell lines, indicating that Tf-modified LP represented a stronger induction of apoptosis on primary acute and chronic leukemia cells.

CD11b is a myeloid cell differentiation antigen. The expression of CD11b was detected by FCM. As shown in Fig. 3E, there was no significant difference in the expression of CD11b between untreated HL-60 and HL-60 administered with blank LP, and the concentration of blank LP had no effect on cell differentiation. The $CD11b^{+}$ percentage in HL-60 cells induced by free As^{III} increased with the increase of As^{III} concentration until 5 μM, the reason for no more differentiated cells is the high concentration of As^{III} ($\geq$ 5 μM) induce a large number of

apoptosis in APL cells. As the cells treated with AsLP and Tf-AsLP, the expression of CD11b on the cell surface increased dose-dependently, when the dosage was 1 μM or more, the percentages of $CD11b^+$ cells for Tf-AsLP group were obviously higher than AsLP group, suggesting that Tf-modified AsLP could enhance the induction of APL cell differentiation by unmodified AsLP.

Since CD71 (TfR-1) was confirmed to highly expressed on the surface of HL-60 cells (as shown on Fig. S3), Tf-modified liposome was applied to entrap As^{III} for the first time to target HL-60 cells which could provide more opportunities for As^{III} to fully interact with APL cells and avoid the toxicity caused by whole body distribution. Tf-modified LP could specifically bind to TfR and significantly increase the uptake of LP by endocytosis, and then As^{III}-containing LP were transported to lysosomes. The acid environment in lysosomes promoted the rapid conversion of Ni $(AsO_2)_2$ into AsO^{2-} and released from the lipid membrane to induce the apoptosis and differentiation of HL-60 cells.

3.4. *In vivo efficacy of Tf-AsLP combined with liposomal RA*

The anti-leukemia efficacy of Tf-AsLP was evaluated using HL-60 subcutaneous tumor model and orthotopic APL model, respectively. Considering that RA is an effective drug to promote differentiation, the combination of RA and arsenic is the gold standard in frontline treatment of APL. In present study, Tf-modified liposomal RA (Tf-RALP) was also prepared basing on the preparation method of Tf-AsLP, and *in vivo* experiments were conducted to study the advantages of combination of two liposome drugs. Two combined administration schemes were set up according to the simultaneous or intermittent regimens in clinic: one was co-administration group (Tf-AsLP + Tf-RALP), the other was sequential administration group (Tf-RALP → Tf-AsLP).

3.4.1. *Anti-tumor efficacy on nude mice bearing HL-60 xenografted tumor*

A secondary transplanted xenografted model was firstly established to evaluate the efficacy of AsLP and Tf-AsLP. After intravenously injected with free As^{III}, AsLP, Tf-AsLP at the As^{III} dose of 0.5 mg/kg or saline every 3 d for 5 times in total (Fig. 5A&5B), the body weight of nude mice kept basically stable during the administration in four groups (Fig. 5C). For saline group, the tumor volume grew rapidly, about 18 times larger at Day 15 after first administration (Fig. 5D). In comparison, AsLP group exhibited a slight tumor inhibition (14.79%). Significantly, Tf-AsLP displayed the best anti-tumor efficacy and the inhibition rates were up to 68.19%. The inhibition rates of As-loaded LP increased by 4.61 times after Tf modification. Then, the tumor tissues were homogenized into cell suspension at 15 d, and stained with APC-labeled anti-human CD11b, then analyzed by FCM (Fig. 5E). $CD11b^+$ cells of Tf-AsLP group accounted for 8.86% ± 2.76%, which was obviously higher than that of AsLP group (3.13% ± 2.27%), indicating that Tf modification improved the ability of AsLP to induce differentiation of APL cells in subcutaneous tumor.

Further, Tf-RALP was prepared and showed uniform particle size, stable ζ-potentials, DL and EE (Table 1). The combination of Tf-RALP and Tf-AsLP was further evaluated on the same model mice. Similarly, the body weight of all mice treated by saline, free drugs, Tf-AsLP and Tf-RALP remained unchanged within treatment (Fig. 5F). As shown in Fig. 5G, the order of growth rate of tumor volume in each treatment group was: saline group>Tf-RALP→Tf-AsLP group >free As^{III}+RA group>Tf-AsLP+Tf-RALP group, the Tf-AsLP+Tf-RALP group displayed the best anti-tumor efficacy, which was more effective than Tf-AsLP injected alone. After introduced Tf-RALP into the co-treatment, the cell proportion of $CD11b^+$ (Fig. 5E) increased to 9.72% ± 3.19%, 1.79 times higher than free drugs sharply, slightly higher than Tf-AsLP group ($P > 0.05$). And co-administration was proved more efficient in cell differentiation induction than sequential therapy (Tf-RALP→Tf-AsLP). Compared with Tf-AsLP group and co-administration group, we inferred that the reduction in the total dose of As^{III} might be one of the reasons for the poor efficacy of sequential group. In addition, studies have shown that RA and As^{III} may have a synergistic effect that RA might improve the anti-cancer activity of As^{III} by promoting uptake, but the specific mechanism is unclear [23].

The histopathology of tissues in subcutaneous model was determined by H&E staining. The liver slices of different groups were shown in Fig. S7A. Free drugs exhibited the strongest hepatotoxicity in all groups, the liver of nude mice was damaged significantly. Severe edema of hepatocytes was observed in the slice, and infiltration of lymphocytes and neutrophils was also observed. AsLP and Tf-AsLP showed less liver toxicity on the slices, presenting less necrosis than that on slices of free drugs. In the groups of synergetic administration, a small amount of APL cells infiltrated in the local hepatic sinuses of the co-administration group. Sequential administration displayed the most serious hepatic damage, along with hemorrhage and infiltration of APL cells in many spots. The spleen slices of different groups were shown in Fig. S7B. In the spleen slices of mice treated with free drugs and sequential administration, extramedullary hematopoiesis, infiltration of APL cells and neutrophils were revealed. In contrast, the co-administration, Tf-AsLP and AsLP reduced the infiltration of APL cells, but still accompanied by hematopoiesis. For safety evaluation, the slices of lung, heart and kidney were also prepared (Fig. S8). The different degree of alveolar walls thickening was occurred in lung slices of nude mice in each group, and the co-administration group showed the closest to the normal lung structure in all six groups. There were no obvious lesions in the heart and kidney of tumor-bearing nude mice. Thus, the results of the efficacy on subcutaneous tumor model could be preliminarily verified that Tf-AsLP reduce the toxicity of free drug for normal tissues and improve the efficacy of AsLP, especially, the combination of liposomal As^{III} and liposomal RA has the potential to improve the efficacy of single administration.

In the process of solid subcutaneous tumor development, the newly formed tumor blood vessels were high in capillary permeability, resulting in AsLP or Tf-AsLP easily penetrating the vascular wall and accumulating in the tumor site to exert efficacy. However, myeloid leukemia was a kind of hematological malignancy, which was mainly developing in BM, instead of a local neoplasm, so that EPR effect was not highly correlated with it. The passive targeting activity of

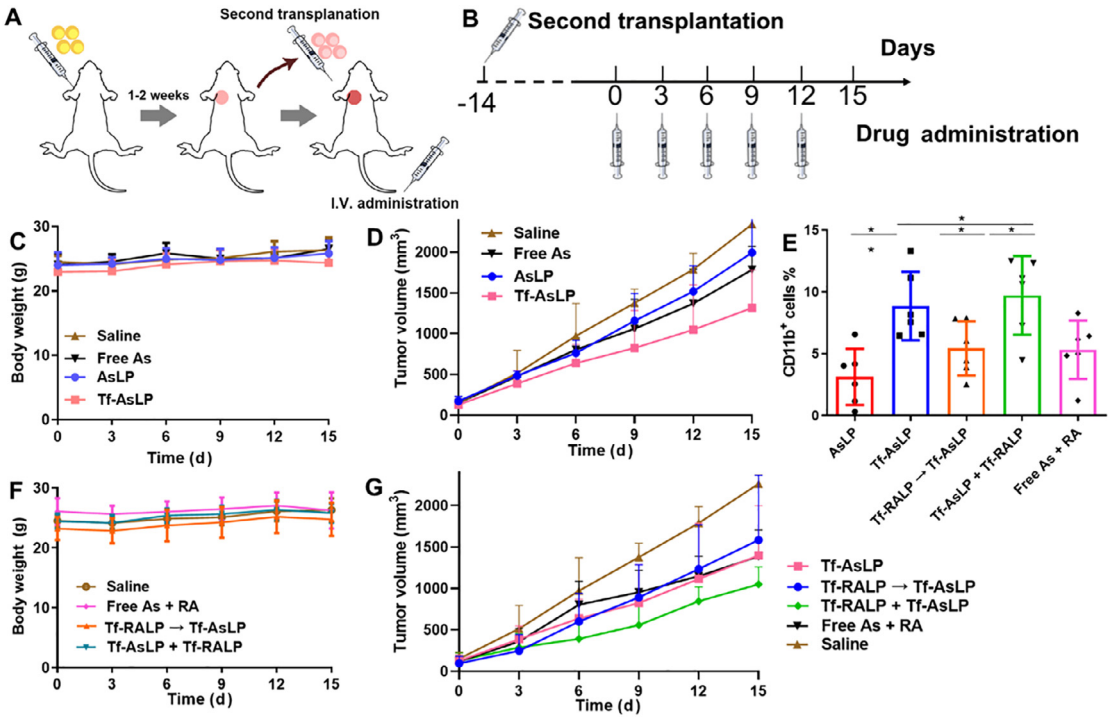

Fig. 5 – *In vivo* efficacy of As-encapsulated liposomes alone or with Tf-RALP on subcutaneous tumor model. Diagram of the establishment (A) and drug administration (B) of subcutaneous tumor-bearing mice. Firstly, body weight (C), tumor volume (D) and CD11b+ cells percentage (E) in the tumor of mice injected As-loaded liposomes alone were collected to evaluate the safety and anti-tumor efficacy. Then, sequential administration (Tf-RALP → Tf-AsLP), co-administration (Tf-RA-LP + TfAsLP) and Free As+RA were intravenously administered at a dose of 0.5 mg/kg As or 1.5 mg/kg RA every 3 days for 6 times in total. Body weight (F), tumor volume (G) and CD11b+ cells percentage (E) were collected for determining the effect of synergetic administration. (*P < 0.05, **P < 0.01, ***P < 0.001).

LP was not fully applicable in the treatment of leukemia. Although the pharmacodynamic study on subcutaneous tumor could not completely represent the effect of LP on leukemia *in vivo*, the effect of Tf-AsLP, Tf-RALP and a series of LP on tumor was still verified to a certain extent.

3.4.2. *In vivo efficacy on APL orthotopic mice model*

In order to further evaluate the efficacy, the APL orthotopic mice model was established, which could successfully simulate the diffuse growth of leukemia and the infiltration into the normal tissues (Fig. 6). NOD/SCID mice were firstly radiated by 2 Gy ^{60}Co followed by intravenously injected HL-60 cells. The blood was taken from the orbit at intervals for cell proportion analyze by FCM. The human-derived CD45$^+$ cells, representing HL-60, accounted for 5.69% ± 0.73% in peripheral blood after 4 weeks, confirming the successful establishment of orthotopic APL animal model [24]. Besides, the BM was also extracted and smeared on the slide for observation under the microscope. As compared with the BM leukocytes of health mice with relatively uniform size and round shape, the BM smears of mice treated by irradiation and APL cell injection displayed many cells with irregular shape, obvious granules in the cytoplasm and larger size, which was similar to the morphological characteristics of HL-60 cells. Thus, it can be proved that APL animals can be obtained by the present modeling method.

After four treatment groups were intravenously injected in APL mice (Fig. 7A), the body weight in free drugs group rapidly reduced from 35th d compared to that of the saline group, and the mortality was the highest, indicating that free drugs were quite toxic and almost ineffective for APL mice. In contrast, the body weight was increased gently after treated with LP and saline, and the percent survival was improved in Tf-AsLP and Tf-AsLP+Tf-RALP groups (Fig. 7B&7C), the survival rates of the four groups were sorted as follows: free As^{III}+RA (14%) < saline (43%) < Tf-AsLP (57%) < Tf-AsLP+Tf-RALP (71%). The treatment of Tf-AsLP+Tf-RALP resulted in the highest survival of APL orthotopic mice, the result was identical with that of the efficacy on the heterotopic tumor mice.

The peripheral blood was taken on the 46th d, and PWBC, RBC and platelet were statistically analyzed by blood routine tests. The reference rage of PWBC in healthy mice was 0.8-6.8 × 10^9/l. As shown in Fig. 7D, the mean PWBC counts of saline, free As^{III}+RA Tf-AsLP and Tf-AsLP+Tf-RALP groups were 13.0 × 10^9/l, 9.4 × 10^9/l, 9.0 × 10^9/l and 6.5 × 10^9/l, respectively. As compared to saline group, free As^{III}+RA group and Tf-AsLP group had about 30% of the inhibition rate of leukemia cells, while the PWBC of co-administration group was already in the normal range, 50% of the inhibition rate was significantly higher than others. In addition, three drug groups had no obvious influences on RBC and platelets of mice according to the several parameters of RBC and platelets

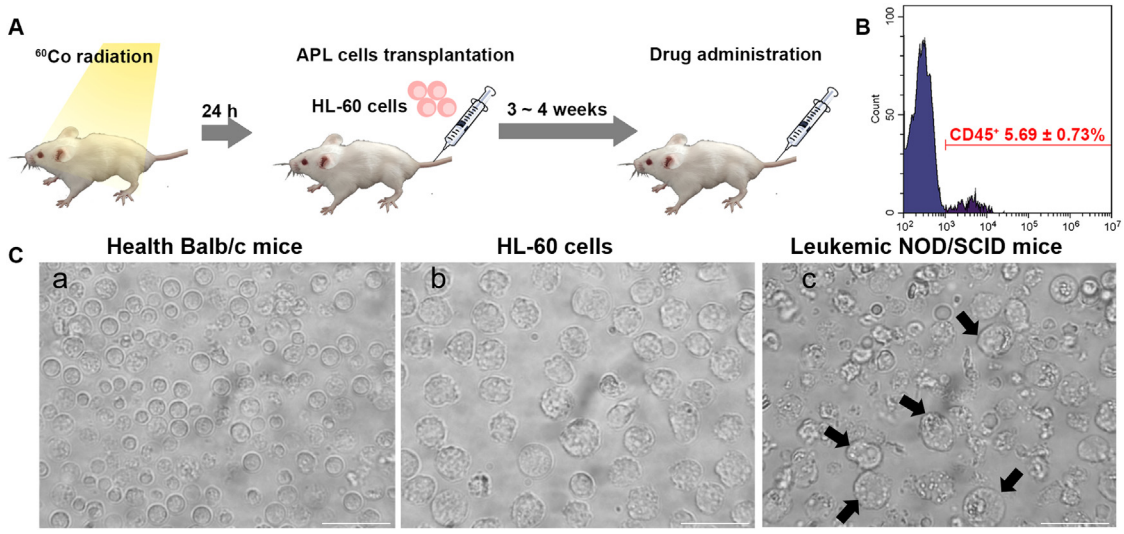

Fig. 6 – APL orthotopic modeling in NOD/SCID mice (A) and flow cytometry profiles of CD45$^+$ cells in peripherical white blood cells (B) after ^{60}Co radiation and HL-60 cells injection. (C) BM smears of health Balb/c mice (a), HL-60 cells (b), APL NOD/SCID mice (c) under microscope (Bar: 40μm). (Black arrow: HL-60 cells in BM of APL NOD/SCID mice).

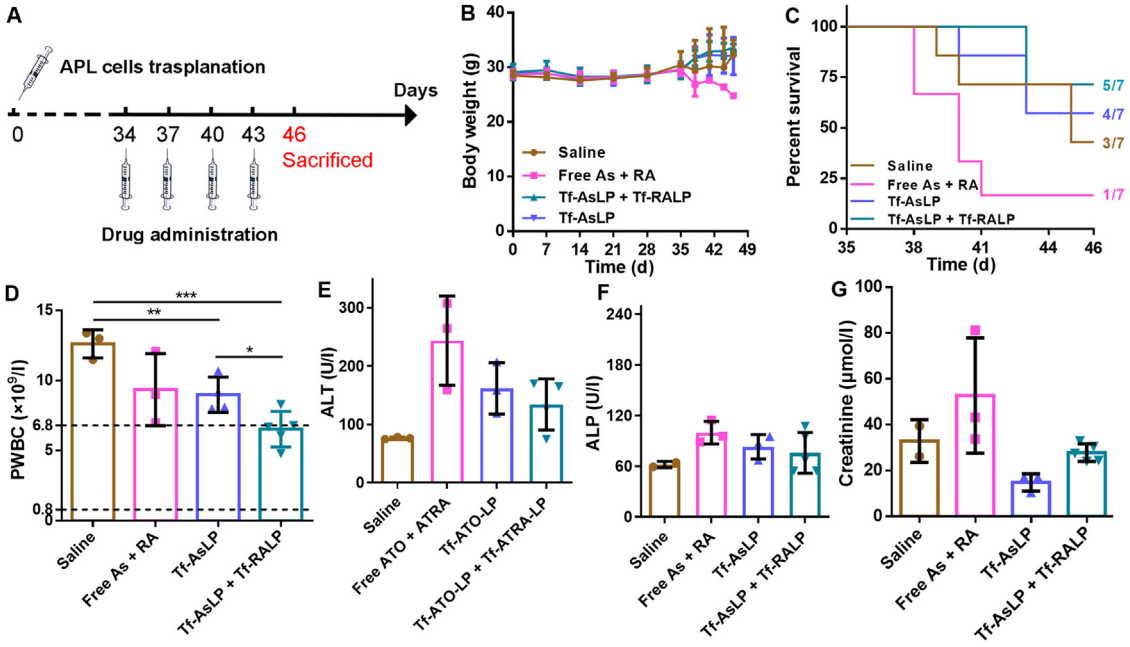

Fig. 7 – *In vivo* efficacy on APL orthotopic model followed the regimen shown in (A) Tf-AsLP, co-administration (Tf-RALP + Tf-AsLP), Free As + RA, and Saline were intravenously administered at a dose of 0.5 mg/kg As or 1.5 mg/kg RA every 3 d for 4 times in total. Body weight (B), percent survival (C), PWBC count (D), serum biochemical indices including ALT (E), ALP (F), Creatinine (G) of NOD/SCID mice at Day 46. (n≥2, *P < 0.05, **P < 0.01, ***P < 0.001).

(Fig. S9). The biochemical indicators of serum including ALT, ALP and Creatinine were analyzed to evaluate the liver and kidney function. ALT and ALP were both increased after free drug treatment, while those in LP groups were lower than that in free drugs group (Fig. 7 E&7F). For creatinine (Fig. 7G), an increase in the value represents the decline in renal function. Free drugs displayed a higher renal toxicity, in contrast, the creatinine level of Tf-AsLP group was about 2 times lower than that of saline group and co-administration group, suggesting that LP could reduce the toxicity of free drugs to liver and kidneys to a certain extent.

In leukemia, BM is one of the predominant sites of tumor localization, delivery of drugs at the BM can improve therapeutic intervention of leukemia. To evaluate the effect of LP on BM, the APL cell count and cell differentiation in BM were determined by FCM (Fig. S10). For the BM samples in saline, free drugs, Tf-AsLP and co-administration groups, the proportions of CD45$^+$ HL-60 cells in BM leukocytes were

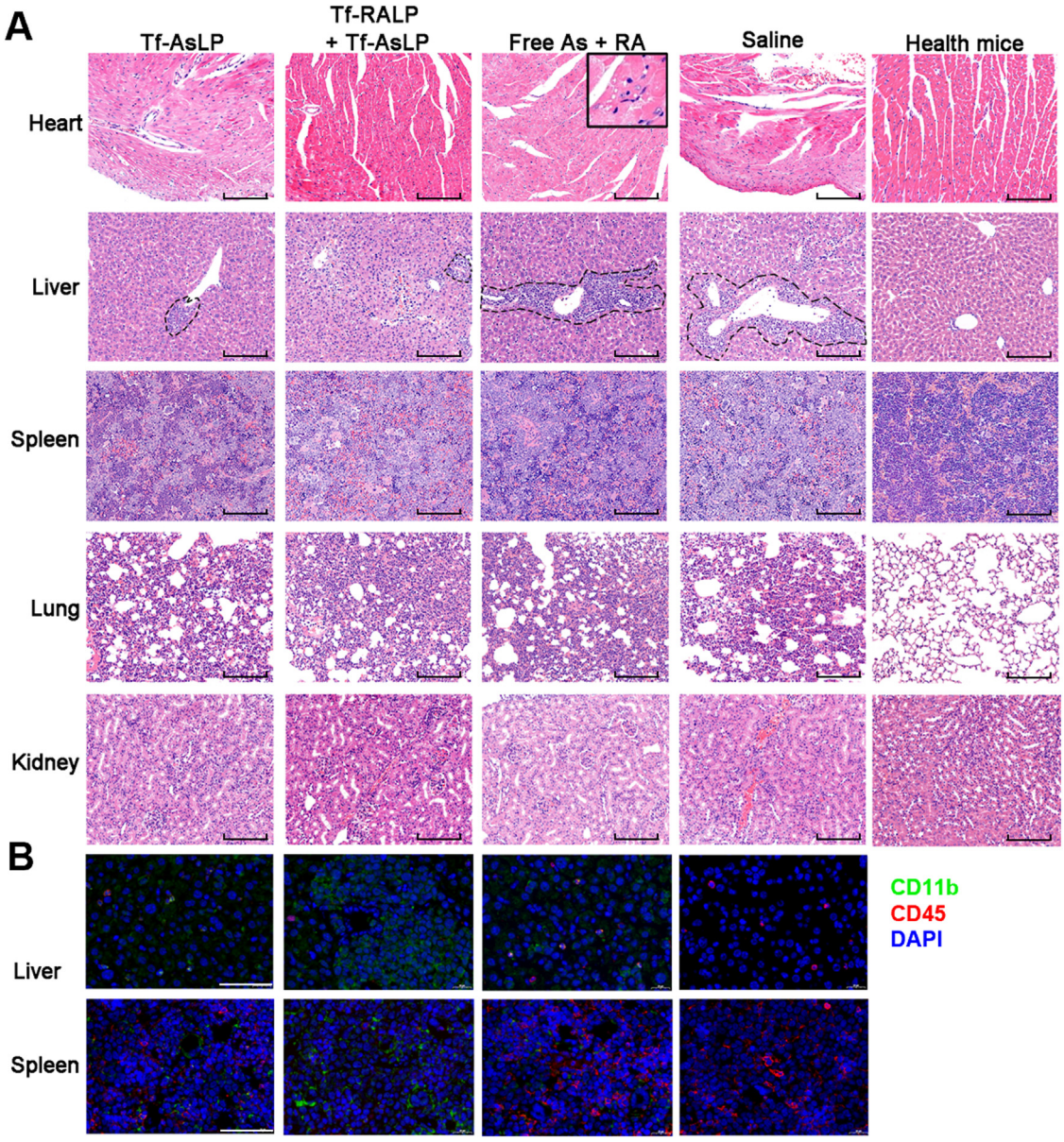

Fig. 8 – The H&E staining of tissues were observed under the microscope (A) (Bar: 200 μm). For examined the infiltration of leukemia cells in tissues, DAPI, CD45 antibody and CD11b antibody were applied to stain the liver and spleen of the mice, and the slices were photographed by CLSM (B). (Bar: 100 μm).

78.52% ± 3.72%, 48.28% ± 13.50%, 65.43% ± 21.96%, and 50.95% ± 7.25%, respectively. Both of free As^{III}+RA group and Tf-AsLP+Tf-RALP group significantly decreased the percentage of $CD45^{+}$ cells compared with saline group, there was no statistical difference between Tf-AsLP and saline, though the average HL-60 count of Tf-AsLP group was lower than that of saline group. On the other hand, the proportions of $CD11b^{+}$ cells in murine BM for free As^{III}+RA and Tf-AsLP+Tf-RALP were obviously higher than saline or Tf-AsLP, indicating the combination of As and RA could markedly inhibit proliferation and promote differentiation of HL-60 cells. The free drugs combination showed the similar effect as the combined LP group, possibly because free drugs with small molecule were more easily distributed in the bone marrow.

The proportion of differentiated cells in murine BM for administration group was higher than that in saline group. Among them, co-administration group and free drug group had the strongest differentiation induction ability, and the proportion of $CD11b^{+}$ cells was obviously higher than that in saline group. In conclusion, Tf-AsLP combined with Tf-RALP exhibited the best efficacy on APL cell inhibition and differentiation *in vivo*, followed by Tf-AsLP.

The histopathology of tissues in orthotopic APL mice was examined by H&E staining, displayed in Fig. 8A. Compared to the health mice, it showed that a large number of leukemic cells were infiltrated in liver of APL mice in saline group and free As^{III}+RA group (seeing dotted line), and the characteristics of diffuse growth were very close to the

occurrence and development of leukemia in clinic. Liposomal treatment reduced the infiltration to a great extent, and the Tf-AsLP+Tf-RALP exhibited the best effect on liver. The co-Tf-AsLP+Tf-RALP group had less infiltration of APL cells in spleen as well. Besides, both Tf-AsLP and Tf-AsLP+Tf-RALP did not show as much cardiotoxicity as free As^{III}+RA. Myocardial fibers in free drugs group were found to be slightly edematous and vacuoles were found in the cytoplasm (seeing the square).

For further study of APL cells infiltration and differentiation, the slices were stained by immunofluorescence (Fig. 8B). The nucleus was dyed with DAPI for blue fluorescence, CD45 was dyed red and CD11b was green. The infiltration of APL cells in spleen was observed more serious than that in liver. The strongest CD45 fluorescence exhibited on the slices of free drug and saline groups, indicating the most serious infiltration of APL cells. With Tf-AsLP alone or co-administration treatment, the APL cells infiltration was significantly reduced in liver and spleen, and the Tf-AsLP+Tf-RALP group showed the minimal infiltration cells. Relatively, the Tf-AsLP injected with Tf-RALP simultaneously displayed the best promotion of APL cell differentiation in liver and spleen, followed by Tf-AsLP. While the free drug only showed a slight effect on cell differentiation.

The analysis of the cells in the peripheral blood and BM found that the free drug in blood was cleared quickly with poor inhibitory effect on the peripheral blood APL cells. The inhibition and differentiation induction in the BM was more significant, possibly because the free As^{III} was easier to enter the BM lumen through the reticuloendothelial sinus capillaries (~60 nm), but free drug also exhibited the highest toxicity with a highest mortality rate of mice in all groups. In contrast, Tf-AsLP alone or in combination with Tf-RALP improved the symptoms of APL mice, manifested by a decrease in the PWBC in peripheral blood and BM and an increase in the differentiation rate of APL cells in BM. Among them, the co-administration of the two LP had the best therapeutic effect on APL mice.

4. Conclusion

Herein, an APL-targeted AsLP was firstly developed. The Tf-AsLP could maintain stable in plasma for relatively long time, and presented a very low As^{III} leakage under normal physiological pH and rapid release in pH 4.5 medium, suggesting lower systemic toxicity and intracellular acid-trigger release in lysosomes. The Tf-AsLP enhanced the uptake of HL-60 cells through the specific binding to TfR on cell surface, stimulated ROS level and Caspase-3 activity to promote apoptosis of APL cells, improved cell differentiation of APL cells to mature cells, also showed significant inhibition on other myeloid leukemia. Tf-AsLP alone or combined with Tf-RALP exhibited inhibitory effect and ability to promote differentiation of APL cells in both subcutaneous tumor and orthotopic model, and co-administration was better than that of single administration and sequential administration. What's more, it was noteworthy that CD71-mediated liposomal arsenic-nickel complex combined with RA could reduce the systemic toxicity and show a better safety than free As^{III} and RA, leading to a great clinical application potential.

Conflicts of interest

The authors declare no conflict of interest.

Acknowledgements

This work was supported by the Science and Technology Commission of Shanghai Municipality (20S11902600), the National Natural Science Foundation of China (82172615) and the PDH-SPFDU Joint Research Fund (RHJJ2018-05)

Supplementary materials

Supplementary material associated with this article can be found, in the online version, at doi:10.1016/j.ajps.2023.100826.

REFERENCES

[1] Adams J, Nassiri M. Acute promyelocytic leukemia: a review and discussion of variant translocations. Arch Pathol Lab Med 2015;139(10):1308–13.
[2] Wang P, Tang Z, Lee B, Zhu JJ, Cai L, Szalaj P, et al. Chromatin topology reorganization and transcription repression by PML-RARalpha in acute promyeloid leukemia. Genome Biol 2020;21(1):110.
[3] Huang ME, Ye YC, Chen SR, Chai JR, Lu JX, Zhoa L, et al. Use of all-trans retinoic acid in the treatment of acute promyelocytic leukemia. Blood 1988;72(2):567–72.
[4] McCulloch D, Brown C, Iland H. Retinoic acid and arsenic trioxide in the treatment of acute promyelocytic leukemia: current perspectives. Onco Targets Ther 2017;10:1585–601.
[5] Frankel SR, Eardley A, Lauwers G, Weiss M, Warrell RP Jr. The "retinoic acid syndrome" in acute promyelocytic leukemia. Ann Intern Med 1992;117(4):292–6.
[6] Hoonjan M, Jadhav V, Bhatt P. Arsenic trioxide: insights into its evolution to an anticancer agent. J Biol Inorg Chem 2018;23(3):313–29.
[7] Zhang XW, Yan XJ, Zhou ZR, Yang FF, Wu ZY, Sun HB, et al. Arsenic trioxide controls the fate of the PML-RARalpha oncoprotein by directly binding PML. Science 2010;328(5975):240–3.
[8] Kumar S, Yedjou CG, Tchounwou PB. Arsenic trioxide induces oxidative stress, DNA damage, and mitochondrial pathway of apoptosis in human leukemia (HL-60) cells. J Exp Clin Cancer Res 2014;33:42.
[9] Shen Z, Chen G, Ni J, Li X, Xiong S, Qiu Q, et al. Use of arsenic trioxide (As_2O_3) in the treatment of acute promyelocytic leukemia (APL): II. Clinical efficacy and pharmacokinetics in relapsed patients. Blood 1997;89(9):3354–60.
[10] Lo-Coco F, Avvisati G, Vignetti M, Thiede C, Orlando SM, Iacobelli S, et al. Retinoic acid and arsenic trioxide for acute promyelocytic leukemia. N Engl J Med 2013;369(2):111–21.
[11] Wang S, Liu C, Wang C, Ma J, Xu H, Guo J, et al. Arsenic trioxide encapsulated liposomes prepared via copper acetate gradient loading method and its antitumor efficiency. Asian J Pharm Sci 2020;15(3):365–73.

[12] Dadashzadeh S, Mirahmadi N, Babaei MH, Vali AM. Peritoneal retention of liposomes: effects of lipid composition, PEG coating and liposome charge. J Control Release 2010;148(2):177–86.
[13] Lyons VJ, Pappas D. Affinity separation and subsequent terminal differentiation of acute myeloid leukemia cells using the human transferrin receptor (CD71) as a capture target. Analyst 2019;144(10):3369–80.
[14] Wang C, Zhang W, He Y, Gao Z, Liu L, Yu S, et al. Ferritin-based targeted delivery of arsenic to diverse leukaemia types confers strong anti-leukaemia therapeutic effects. Nat Nanotechnol 2021;16(12):1413–23.
[15] Li Y, Ruan S, Guo J, He Z, Xia Q, Wu T, et al. B16F10 cell membrane-based nanovesicles for melanoma therapy are superior to hyaluronic acid-modified nanocarriers. Mol Pharm 2022;19(8):2840–53.
[16] Zhang Y, Xia Q, Wu T, He Z, Li Y, Li Z, et al. A novel multi-functionalized multicellular nanodelivery system for non-small cell lung cancer photochemotherapy. J Nanobiotechnol 2021;19(1):245.
[17] Nandi U, Onyesom I, Douroumis D. Transferrin conjugated Stealth liposomes for sirolimus active targeting in breast cancer. J Drug Delivery Sci Technol 2021;66:1–8.
[18] Burnett AK, Russell NH, Hills RK, Bowen D, Kell J, Knapper S, et al. Arsenic trioxide and all-trans retinoic acid treatment for acute promyelocytic leukaemia in all risk groups (AML17): results of a randomised, controlled, phase 3 trial. Lancet Oncol 2015;16(13):1295–305.
[19] Platzbecker U, Avvisati G, Cicconi L, Thiede C, Paoloni F, Vignetti M, et al. Improved outcomes with retinoic acid and arsenic trioxide compared with retinoic acid and chemotherapy in non–high-risk acute promyelocytic leukemia: final results of the randomized Italian-German APL0406 trial. J Clin Oncol 2017;35(6):605–12.
[20] Powell JA, Lewis AC, Zhu W, Toubia J, Pitman MR, Wallington-Beddoe CT, et al. Targeting sphingosine kinase 1 induces MCL1-dependent cell death in acute myeloid leukemia. Blood 2017;129(6):771–82.
[21] Chen H, MacDonald RC, Li S, Krett NL, Rosen ST, O'Halloran TV. Lipid encapsulation of arsenic trioxide attenuates cytotoxicity and allows for controlled anticancer drug release. J AM Chem Soc 2006;128:13348–9.
[22] Yedjou C, Tchounwou P, Jenkins J, McMurray R. Basic mechanisms of arsenic trioxide (ATO)-induced apoptosis in human leukemia (HL-60) cells. J Hematol Oncol 2010;3:28.
[23] Kozono S, Lin YM, Seo HS, Pinch B, Lian X, Qiu C, et al. Arsenic targets Pin1 and cooperates with retinoic acid to inhibit cancer-driving pathways and tumor-initiating cells. Nat Commun 2018;9(1):3069.
[24] Rego EM, He LZ, Warrell RP Jr, Wang ZG, Pandolfi PP. Retinoic acid (RA) and As_2O_3 treatment in transgenic models of acute promyelocytic leukemia (APL) unravel the distinct nature of the leukemogenic process induced by the PML-RARalpha and PLZF-RARalpha oncoproteins. Proc Natl Acad Sci USA 2000;97(18):10173–8.